Nat Hazards (2010) 55:123–144
DOI 10.1007/s11069-010-9563-0

ORIGINAL PAPER

Stochastic methods for safety assessment of the flood defense system in the Scheldt Estuary of the Netherlands

Mohammadreza Rajabalinejad · Tewfik Mahdi · Pieter van Gelder

Received: 22 December 2009 / Accepted: 27 May 2010 / Published online: 14 July 2010

Abstract In this study, we address the effective method to apply a novel reliability method integrated with finite element models to the safety assessment of pilot site Scheldt in the Netherlands. This site was considered as one of the three main pilot sites in Europe to assess the application of newly suggested techniques in order to reduce and manage the flood risk in the Floodsite project. http://www.floodsite.net, 2004–2009). The novel method of dynamic bounds (DB) is applied to this site after a successful experience in (Rajabalinejad in Reliability methods for finite element models, 1 edn. IOS Press, Amsterdam, 2009). In this study, the bi-functional response of the finite element model is considered, and the dimensional uncertainty is defined presenting the expected uncertainty for a certain dimension in the DB method. The uncertainty is used as a judgment tool to choose the dimension for the DB method for the desired accuracy. The results obtained by applying this technique are presented in this paper.

Keywords Reliability · Monte Carlo · Dynamic bounds · Flood defense · Monotonic

1 Introduction

Failure of flood defense structures can endanger humans and environment, resulting in casualties, loss of life and economical damages. These structures are also becoming more important to engineers, inhabitants and decision makers with the increasing trend in the global warming and sea levels rise (SLR) that lead to higher storm surges and increase the flood risk (van Gelder et al. 2008; Demirbilek et al. 2009; Vicksburg 2008; Demirbilek et al. 2010). This importance is more evident after the failure of an extensive network of

M. Rajabalinejad (✉) · T. Mahdi
Department of Civil, Geological and Mining Engineering, Ecole Polytechnique Montreal, Montreal, Canada
e-mail: M.Rajabalinejad@polymtl.ca

P. van Gelder
Hydraulic Engineering Department, TUDelft, Delft, The Netherlands

different type of flood defense structures all over the world. An example of failure of the flood defense system happened in New Orleans during Hurricane Katrina (Link et al. 2006; USACE-b 2006; Demirbilek et al. 2010). This city was protected by a system of levees, flood walls and barriers. The New Orleans flood protection system is a typical example that shows a flood defense system behaves like a serial system, and that all of its elements must be reliable and not fail in order for the overall system to meet its requirements. In other words, the operational reliability of each element of a flood defense system should be accurately assessed by utmost consideration of the consequences of any component failure in the system. Therefore, more resilient flood defenses will be required in the future to meet these demands and potential failures of systems caused by episodic extreme metocean events (meteorological and atmospheric). This realization has prompted many research studies to investigate accurate safety requirements for the flood defenses. The European Union's FloodSite project is an example of this high-priority research and an evidence of a collective attempt of 37 leading European institutes to reduce the risk of flooding in the homelands. This project was supported by the Parliament and Council of the European Union to address a new European guidelines for assessment and management of flood risks. It commenced in 2004 and runs to 2009. This integrated project covers the physical, environmental, ecological and socio-economic aspects of floods from rivers, estuaries and the sea. Key issues that are addressed in this project are hazard sources and consequences of flooding on people, property and the environment.

The process of flood risk management is one of the important issues that includes risk mitigation measures, preparedness, emergency plans for flood management actions during and after an event at the project site. Since floods often cross international borders, the risk management schemes are universal. Many research studies have been considered for rivers, estuaries and coastal sites in Belgium, the Czech Republic, France, Germany, Hungary, Italy, the Netherlands, Spain and the UK. These pilot studies leaded FloodSite program dealt with real and specific problems upon which knowledge, methods and tools were developed and tested. This project is divided into 32 tasks of which Task 4 and Task 7 provide the building blocks of the risk assessment process. Task 4 in this project addresses a detailed overview of the expected scenarios of failure of different flood defense structures (Morris 2009), and Task 7 integrates these expected scenarios and provides a reliability tool (van Gelder 2009). There are three pilot sites defined for these tasks to apply and evaluate new techniques: River Elbe Basin in Germany, River Thames Estuary in England and River Scheldt Estuary in the Netherlands. The Scheldt pilot site is shown in Fig. 1. The suggested methods evaluated at this project are straightforward and easy to follow, but sometimes they are not accurate and have shortcomings (Rajabalinejad et al. 2009).

One weakness of this research project is the lack of integration of different failure scenarios and failure modes in a reliable model. To bridge this gap, two issues must be addressed: an accurate model for load–resistance characteristics of the system and an appropriate reliability method for risk/failure behavior of the system, for which the probabilistic finite element models offer one of the best complementary solution. Nevertheless, this approach is costly because many analyses are required to evaluate different aspects of model outcomes and the role of different input variables used in the PFE models. In other words, adaptation of such an integrated approach leads to a very time-consuming process that is not practice-oriented. In this paper, we provide a computational framework and demonstrate implementation of novel methods for solving a challenging problem in assessment of safety of infrastructures.

The layout of this paper is as follows. Section 2 introduces the framework of the problem and briefly describes the suggested solutions. The monotonic property, as a

Fig. 1 The plan view of the Scheldt estuary, the white area is called "Zeeuwsch Vlaannderen" and is counted as Dike Ring 32 in the flood protection system of the Netherlands (Googleearth)

requirement for the dynamic bounds method, is presented in Sect. 3. The reliability methods that are used in this paper are discussed in Sect. 4. The implemented theory for the current calculation of probability of failure of sliding in the Scheldt pilot site is presented in Sect. 5. Two typical cross-sections of Scheldt demonstration site are addressed in Sects. 6 and 7. Sections 8–10 provide results for the currently applied method, Monte Carlo method and DB method, respectively. In the latter section, we introduce the dimensional uncertainty and show its implementation to manage the dimensionality of problem. Results are compared in Sect. 11. Section 12 presents concluding remarks of this research.

2 Problem statement

Evaluating the reliability of a flood defense system is a challenging task because of different possible failure scenarios and failure modes (van Gelder 2009; Morris 2009). Approximate methods via the first-order reliability method provide efficient ways of evaluating failure probability of the "most probable" failure. The trade off is that the failure probability estimates may be biased toward the unconservative side. The Monte Carlo simulation (MCS) is a viable unbiased way of estimating the failure probability of a dike, but MCS is inefficient for problems with small failure probabilities. This study proposes a novel way based on the dynamic bounds that can be integrated with importance sampling technique for calculating failure probabilities to estimate reliability that is unbiased and yet is much more efficient than MCS. In particular, the critical issue of the dimensionality of DB method is addressed in detail. The model developed is used in examples to demonstrate the performance of the new method.

To calculate failure probabilities of flood protection systems, we will focus our attention on implementation of probabilistic finite elements (PFEs) in the Monte Carlo (MC) methods. This is necessary because Monte Carlo methods are flexible and best suited for dealing with such complicated problems. The Monte Carlo family of methods includes the so-called variance optimization schemes for improving the computational efficiency. Among these, the most widely used are the importance sampling (IS), as explained in (Melchers 1999) and directional sampling (DS) presented in (Nie and Ellingwood 2000) and some recently developed methods such as Bayesian Monte Carlo (BMC) presented in (Rajabalinejad 2010; Rajabalinejad and Mahdi 2010), dynamic bounds (DB) described in (Rajabalinejad 2009) and improved dynamic bounds (IDB) presented in (Rajabalinejad et al. 2010a) . Each method has its advantages and disadvantages when it is coupled with finite elements. These existing methods have been discussed in (Rajabalinejad 2009), but the probabilistic finite elements approach is still a time-consuming process and difficult to apply to the routine engineering works. To address this problem, we apply the novel method of dynamic bounds (DB) to the pilot site Scheldt. The purpose of DB technique is to improve the computational efficiency of finite element numerical models used in calculation of failure analyses of coastal structures. Depending on the particulars of an application, the DB method may speed up the overall simulation process by several orders of magnitude. It is shown in (Rajabalinejad 2009, see tables 3.3 and 3.6) that for applications controlled by two and four influential variables (e.g, two-dimensional and four-dimensional problems), the computational efficiency can be improved by factors of 130 and 9, respectively.

The concept of monotonicity[1], a requirement for the methods of DB, is described in Sect. 3.

The pilot site Scheldt is modeled by finite elements using the Plaxis code. The finite element code is integrated with the DB method to develop generalized model applicable to complex flood defense structures. The results are compared to estimates from Monte Carlo method, the technique presently used at the pilot site for the sliding process. The sliding failure mechanism that can occur in different modes is one of the important scenarios for failure of the Scheldt flood defense system. This significant failure scenario is briefly discussed in Sect. 2.1. The Bishop method is integrated with the random field theory and tested in the pilot site. Practical solutions for the safety assessment of flood defenses are developed in this research for the sliding mechanism.

2.1 Sliding

The stability analysis of slopes is challenging because failure mode and shape for a slope depend on the geometry, boundary conditions, soil parameters and their variations. The determination of variables such as the soil stratification and the variation of the in-place strength parameters further increase the complexity of a problem. The water seepage through the slope and the choice of a potential slip surface adds more to the complexity of problem. In general, sliding of a slope may occur partially toward the landside, pool-side or the whole system; these three modes of failure are sketched in Fig. 2.

Different methods available to analyze the stability of a slope and assess its safety factor, defined as the ratio of resistant forces to driving forces. These methods can be divided into two categories: analytical and numerical (usually finite element) methods. Analytical methods are based on the physical modeling of soil behavior and an imposed failure shape, which can be circular or none circular. The method of Bishop, which considers a circular failure shape, is one of the most widely used methods in stability of

[1] It means the monotonic behavior of the limit state equation used in a finite element model in our case.

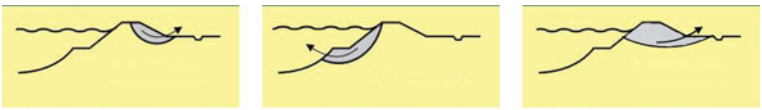

Fig. 2 Types of sliding for dikes; **a** partial sliding toward the land side, **b** partial sliding toward the pool side and **c** sliding of the whole system (dike or levee)

slopes (Baker and Garber 1978). Finite element methods are generally more flexible, versatile and reliable (Griffiths and Lane 1999). For sliding failure, the finite element analysis provides several advantages when compared to the analytical approach. For example, there is no need to define a failure shape from the beginning because the solution provides the most probable failure shape according to the maximum deformation of nodes. Furthermore, there is no need to consider separate failure modes since finite element models integrate all failure modes. For these reasons, the finite element analysis is a more realistic approach for calculating the reliability of slopes.

3 Monotonicity

Engineering problems exhibit some form of monotonicity. For example, a larger load on a structure means a smaller safety margin or possibly failure; strengthening the structure typically increases the safety margin. There are many examples of such monotonic behavior. Therefore, assuming a monotonic limit state equation does not reduce the scope of application or applicability of the state equation.

A function is called *increasing* with respect to a variable if its value rises as the variable increases, regardless of the values of the other variables. If the function decreases in this situation, one says that the function is *decreasing* with respect to the variable. A function is called *monotonic*, if for each of its variables, it is either increasing or decreasing.

More formally, a limit state equation G is called monotonic if, for each i, and for each choice of $x_1, x_2, \ldots, x_{i-1}, x_{i+1}, \ldots, x_n$, the function h_i defined as

$$h_i(x) = G(x_1, x_2, \ldots, x_{i-1}, x, x_{i+1}, \ldots, x_n)$$

is either increasing (i.e., $x \leq y$ implies $h_i(x) \leq h_i(y)$) or decreasing (i.e., $x \leq y$ implies $h_i(x) \geq h_i(y)$). Note that this definition also includes functions that may not be *strictly* increasing (Rajabalinejad 2009).

4 Reliability methods

In this section, we present a brief description of the reliability methods used in this paper, the first-order reliability method (FORM), method of Monte Carlo (MC) and dynamic bounds (DB). FORM is well explained in the literature, see for instance (Melchers 1999, Choi et al. 2006). MC is also a very well-established technique and different applications of this method are given in (Fishman 1996). Since MC is the fundamental part of the novel technique of DB, a brief description of MC and DB methods is presented. The algorithm of DB is briefly described in Sect. 4.2.

4.1 Monte Carlo method

For the mathematical formulation and implementation features of DB in the Monte Carlo method, we assume a limit state equation $G(\mathbf{x})$ is given, where $\mathbf{x} = (x_1, \ldots, x_n)$ represents the vector of relevant parameters, and n is the dimension of the problem (for purposes of illustration sometimes n is assumed 2). The parameters are treated as a random vector $\mathbf{X} = (X_1, \ldots, X_n)$, whose joint probability density function f is known. Given that $G(\mathbf{x}) < 0$ corresponds to failure, we define the probability of failure as

$$p_{\mathrm{f}} = \mathrm{P}(G\mathbf{X}) < 0 = \int \ldots \int_{\mathbf{x}:G(\mathbf{x})<0} f(\mathbf{x})\mathrm{d}\mathbf{x}.$$

In the Monte Carlo approach, we consider N independent discrete replications $\mathbf{X}_1, \ldots, \mathbf{X}_N)$ of $\mathbf{X}$ to define an estimate of p_f as

$$\hat{p}_{\mathrm{f}} = \frac{1}{N}\sum_{i=1}^{N} \mathbf{1}[G(\mathbf{X}_i) < 0], \tag{1}$$

where $1[C]$ equals $\mathbf{1}$ if condition C is true and 0 otherwise. This procedure would require N evaluations of the limit state equation (G). However, in many situations G increases in some variables and decreases in others, and this behavior can be exploited to reduce the number of times $G(\mathbf{x})$ should be evaluated. Integrating the prior information into the standard method is the principle most that guided us to develop the dynamic bounds method.

4.2 Dynamic bounds (DB)

In the reliability analysis of engineering problems, dynamic bounds (DB) is introduced for the monotonic limit state equations (LSEs) with a limited number of influential variables. The application of this method for a complex flood defense structure is presented in (Rajabalinejad et al. 2010b). DB takes into account monotonicity, some typical prior information on characteristics of LSEs for engineering problems, in order to reduce the calculation efforts in the Monte Carlo process. The DB method divides the range of a LSE into three regions of stable, unstable and unqualified, for speeding up the Monte Carlo process as is shown in Fig. 3. This division improves the calculation efficiency by gradually decreasing the size of the unqualified region. The algorithm of this technique is described in the following section.

4.2.1 Algorithm of dynamic bounds

In Fig. 3, a two-dimensional limit state equation $G(x_1, x_2) = 0$ is depicted, with the contours of joint probability density function $f(x_1, x_2)$ for two variables (X_1, X_2). The limit state equation $G(x_1, x_2)$ is assumed to be monotonically increasing in both variables. The first random point, $\mathbf{x}^{(1)} = (x_1^{(1)}, x_2^{(1)})$, is generated from the joint probability distribution function (JPDF) f. In Fig. 3, it is depicted by a black square (labeled 1), for which $G(x_1^{(1)}, x_2^{(1)}) < 0$, representing a failure point in the unstable region to the left of and below $(x_1^{(1)}, x_2^{(1)})$. In the next step, the point $(x_1^{(2)}, x_2^{(2)})$ is generated from f, such that $G(x_1^{(2)}, x_2^{(2)}) > 0$. Hence, point 2 is in the stable region, and all points in the right-upper quadrant from point 2 are stable as well. This process is repeated and the result of a small

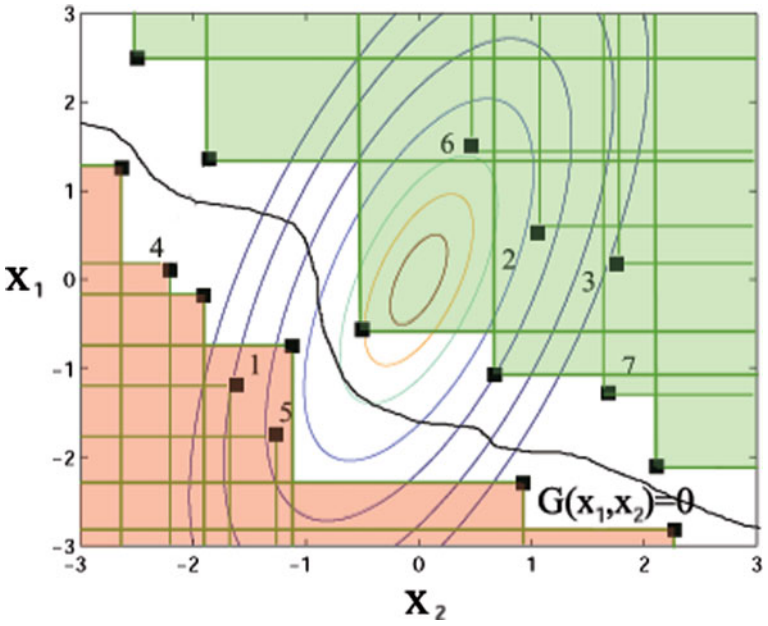

Fig. 3 Illustration of the dynamic bounds algorithm in which a two-dimensional joint probability density function is divided into the stable, unstable and unqualified regions

number of iterations is shown in Fig. 3. The shaded regions constitute approximations to the stable and unstable regions that can be used to obtain bounds for the probability of failure p_f.

For a limit state equation of dimension n, we define the stable set S and the unstable set U as

$$S = \{\mathbf{x} : G(\mathbf{x}) \geq 0\} \quad \text{and} \quad U = \{\mathbf{x} : G(\mathbf{x}) < 0\}. \tag{2}$$

If two points $\mathbf{x} = (x_1, \ldots, x_n)$ and $\mathbf{y} = (y_1, \ldots, y_n)$ satisfy the relationship $x_i \leq y_i$ for $x = (1, \ldots, n)$, then we say that $\mathbf{x}$ is *less stable than* $\mathbf{y}$, or $\mathbf{y}$ is *more stable than* $\mathbf{x}$. If $\mathbf{x} \in S$, then $\mathbf{y} \in S$ follows, and a similar statement holds for U as well.

Consider the kth iteration of the Monte Carlo process. A number of stable points, say, $\mathbf{s}^{(1)}, \ldots, \mathbf{s}^{(p)}$ and a number of unstable points $\mathbf{u}^{(1)}, \ldots, \mathbf{u}^{(q)}$ have been generated. The current approximation to the stable region S is the union of the p orthants, and by generalizing the quadrants in Fig. 3 we show

$$H_i = \{\mathbf{x} : \mathbf{x} \text{ is more stable than } \mathbf{s}^{(i)}\}, \quad i = 1, \ldots, p. \tag{3}$$

If $\mathbf{s}^{(i)}$ is more stable than $\mathbf{s}^{(j)}$, for some i and j, its orthant H_i is completely contained in H_j, and there would be no loss of information if $\mathbf{s}^{(i)}$ were dropped from the list of points. Similarly, the current approximation to the unstable region U is the union of

$$L_i = \{\mathbf{x} : \mathbf{x} \text{ is less stable than } \mathbf{s}^{(i)}\}, \quad i = 1, \ldots, q. \tag{4}$$

From now on, we assume that only a minimal set of stable and unstable points is retained during the simulation, and S_k and U_k are the corresponding approximations to S and U:

$$S_k = \cup_{i=1}^{p} H_i \quad \text{and} \quad U_k = \cup_{i=1}^{q} L_i. \tag{5}$$

Now, imagine the next random point $\mathbf{X}^{(k+1)}$ is generated from f. There are three possibilities. First, $\mathbf{X}^{(k+1)} \in S_k$, indicating the point is located in a region of the stable set. Second, $\mathbf{X}^{(k+1)} \in U_k$, such that the point is located in a region of the unstable set requiring the count of the number of failures to be incremented. Third, $\mathbf{X}^{(k+1)} \notin S_k \cup U_k$, and the point is located in the unqualified region between S_k and U_k necessitating evaluation of $G(\mathbf{X}^{(k+1)})$. If it is positive, $\mathbf{X}^{(k+1)}$ is added to the collection of known stable points, and this collection may also be checked for its minimality, dropping any superfluous points. If it is negative, $\mathbf{X}^{(k+1)}$ is added to the collection of unstable points and a similar update is performed. Note that the numbers p and q vary during the simulation and depend on the iteration number k.

In Summary, the algorithm is as follows:

1. Determine S_0 and U_0. These can be empty sets or determined from the threshold points, as described. Set $k = 0$, $n_f = 0$.
2. Increase k by 1 and generate $\mathbf{X}^{(k)}$ from f. If $\mathbf{X}^{(k)} \in U_{k-1}$, add 1 to n_f and update U_{k-1} to obtain U_k. If $\mathbf{X}^{(k)} \notin S_{k-1} \cup U_{k-1}$, evaluate $G(\mathbf{X}^{(k)})$, and if it is negative, add 1 to n_f and update U_{k-1} to obtain U_k; otherwise, update S_{k-1} to obtain S_k. Repeat until $k = N$.
3. Calculate $\hat{p}_f = n_f/N$ as the Monte Carlo estimate for p_f.

This estimate $\hat{p}_f$ is as good as an ordinary Monte Carlo estimate based on N independent samples $\mathbf{1}[G(\mathbf{X}^{(1)}) < 0], \ldots, \mathbf{1}[G(\mathbf{X}^{(N)}) < 0]$. However, it requires evaluation of G using only a fraction of the samples.

5 Implementing the spatial variation of parameters

The estimation of probability of sliding in the FloodSite project uses analytical methods and random field theory as implemented in Mprostab program for the pilot site Scheldt. Mprostab is programmed in GeoDelft. This approach is also used in PC-Ring for safety assessment of dike rings in the Netherlands. In this section, we briefly describe the implemented theory. This presentation is based on (Calle 1994), and further information is available in this reference.

The variation of soil parameters follows a lognormal distribution. We start with a brief introduction to lognormal distribution and provide further theoretical and practical information about implementation of random field theory for these types of problems.

5.1 Lognormal distribution

Variations in soil parameters are usually considered according to the normal or lognormal distribution. A normal probability density function (PDF) of a variable, X, is defined as

$$f_X(x) = \frac{1}{\sqrt{2\pi}\sigma} \exp\left(-\frac{(x-\mu)^2}{2\sigma^2}\right), \tag{6}$$

where μ and σ are respectively mean and the standard deviation, and x is a random sample (scalar value). A lognormal PDF is obtained if the random sample x from a normal random variable X is replaced by $\ln(x)$. The parameters of a lognormal distribution can be obtained from the following equation:

$$f_X(x) = \frac{1}{\sqrt{2\pi}\sigma_{\ln X}} \exp\left(-\frac{(\ln x - \mu_{\ln X})^2}{2\sigma_{\ln X}^2}\right), \tag{7}$$

where $\mu_{\ln X} = E[\ln(X)] = \ln\left(\mu_X - \frac{1}{2}\sigma_{\ln X}^2\right)$, and $\sigma_{\ln X}^2 = Var[\ln(X)] = \ln\left(1 + \left(\frac{\sigma_X}{\mu_X}\right)^2\right)$.

The advantage of a lognormal PDF is that it always yields positive values while there is always possibility of yielding negative values by a normal PDF. However, there is not a big difference for small ratios of the mean value and standard deviation, $\frac{\mu_x}{\sigma_x}$. A comparison of the normal and lognormal PDF is given in (Griffiths and Fenton 2007). In order to take into account the spatial variation of soil parameters, PDF of soil parameters and an auto correlation function are required.

5.2 Modified autocorrelation function

The autocorrelation function defines correlation between possible values at two points within a soil layer. A weak stationary property is assumed to ensure that the marginal PDFs are identical, and correlation among two points is only a function of distance lag (τ). The modified autocorrelation function of Gaussian type is used as

$$\rho(\delta_x, \delta_y, \delta_z) = e^{-\frac{\delta_x^2 + \delta_z^2}{D_h^2}}((1-\alpha) + \alpha e^{-\frac{\delta_y^2}{D_v^2}}). \tag{8}$$

This autocorrelation function is a function of distance between two points. Here, x and z are horizontal, and y is vertical spatial coordinate. The distance between two points is $\delta_x = |x_1 - x_2|$, $\delta_y = |y_1 - y_2|$, and $\delta_z = |z_1 - z_2|$. D_h and D_v are, respectively, called the horizontal and vertical correlation length. The correlation length in horizontal direction is greater than the vertical. A range of 25–100 m for the horizontal correlation length and 0.1–3 m for vertical direction is assumed (Calle 1994). The variance parameter α is equal to ratio of local and total variance and is defined as

$$\alpha = \frac{\sigma_{\text{vertical}}^2}{\sigma_{\text{total}}^2}. \tag{9}$$

For $\alpha = 1$, the autocorrelation function is the classical Gaussian form. This parameter enables consistent modeling of the presence of overall weak and strong locations within a layer. Values of α ranging between 0.5 and 1.0 (Calle 1994).

Parameters of the probability distributions are the expected mean values and standard deviations. These are usually estimated on the basis of series of laboratory or in situ test data. Since the samples are finite, estimators are statistically biased. A bias estimator is a source of uncertainty, and Mprostab takes this uncertainty into account by adjusting the field variance with a factor $\frac{n+1}{n}$ and modifies the autocorrelation function (Vanmarcke 1983; Calle 1994) as

$$r(\delta_x, \delta_y, \delta_z) = \frac{n}{n+1}\rho(\delta_x, \delta_y, \delta_z) + \frac{1}{n+1}. \tag{10}$$

5.3 Bishop technique

The slope stability problems are modeled assuming physical equilibrium between parameters that are statistically undetermined. Simplifying assumptions are necessary, leading to development of different methods. The popular methods are those developed by Fellenius, Bishop, Janbu and Spencer (Malkawi et al. 2000; Lacasse et al. 2007). Here, we consider the simplified Bishop model that satisfies only the overall moment and is

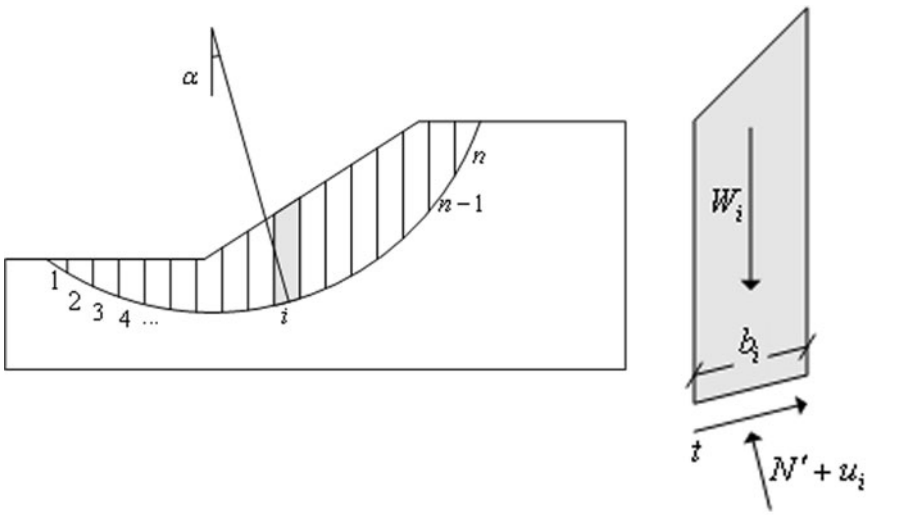

(a) The Bishop method **(b)** Internal forces on each slice

Fig. 4 A schematic representation of the Bishop method is presented, and the internal forces on each element are shown

applicable to a circular slip surface. This approach is used in the pilot site Scheldt. For the Bishop model, the factor of safety is directly obtained by assuming inter slice forces are parallel to the base of each slice that can be neglected (see Fig. 4). On the basis of Bishop Method, the limit state equation is defined in (Calle 1994) as

$$Z = M_r - q \times M_0, \tag{11}$$

where resistance and driving moments are respectively called as M_0 and M_r. A stochastic parameter (q_i) is used in the model, it is called the model factor with an expected value μ_q and standard deviation σ_q. According to Bishop method, the resistance moment is obtained by

$$M_r = \frac{\sum_{i=1}^{n} \left\{ \frac{c_i'}{F} + (W_i - b_i u_i) \frac{\tan \phi_i'}{F} \right\}}{\left\{ \cos \alpha_i + \sin \alpha_i \frac{\tan \phi_i'}{F} \right\}}, \tag{12}$$

where F is the safety factor, u is the water pressure, c and ϕ are the soil parameters, and W is the weight of the slice (Fig. 4). The driving moment is the total weight of each slice given as

$$M_0 = \sum_{i=1}^{n} W_i \sin \alpha_i. \tag{13}$$

Considering the variation of soil parameters, water level and the model factor, the first-order estimation of the limit state equation at the expected point is obtained as

$$Z_l = Z(c_0, t_0, u_0, q_0) + \nabla_c^T Z(c - c_0) + \nabla_t^T Z(t - t_0) + \nabla_u^T Z(u - u_0) + \nabla_q^T Z(q - q_0), \tag{14}$$

where ∇ and T, are respectively, the gradient and transpose signs. Z_l is a random variable that may be estimated by its first and second moment ($E[Z_l]$ and $\sigma^2[Z_l]$). Given the first and

second moment of the first-order extension of the limit state equation, the reliability index can be obtained as

$$\beta = \frac{E[Z_l]}{\sigma(Z_l)}, \tag{15}$$

which leads to the estimated probability of failure by

$$P[Z<0] \approx P[Z_l<0] = \Phi(-\beta), \tag{16}$$

where Φ is the probability that the random variable does not exceed a design value by assuming the standard normal distribution, (ϕ_N) defined as

$$\varphi_N(u) = \frac{e^{(\frac{u^2}{2})}}{\sqrt{2\pi}\sigma_X}, \tag{17}$$

where $u = \frac{x-\mu_X}{\sigma_X}$.

5.4 Finite elements

Finite element analysis is a technique for solving partial differential equations by discretizing the equations in spatial dimensions. This discretization can be done using different element shapes and a finite number of elements. A matrix can be constructed to relate the inputs to the outputs on some specific points that are called nodes. The system of equations are solved relating the inputs and outputs by partial differential equations. The average variation of soil layers is considered in the finite element analysis. Further information on the method and its applications can be found in (Smith and Griffiths 2004; Haldar and Mahadevan 2000).

6 Example application: Pilot site Scheldt

Located in the Netherlands, the Scheldt pilot site is a typical North Sea area protected against coastal flooding by different flood defense structures. Flood is the dominant hazard in the Netherlands, and most of the areas are protected by forelands, levees, dikes, dunes, barriers and other flood defenses. The Western Scheldt forms the entrance to the harbor of Antwerp (Belgium). Water levels are influenced by the wind surges on the North Sea, as well as the river discharges from the Scheldt. Among the elements of the protection system, the dike rings play a key role because of their importance, function and their contribution to the system. Dike rings are divided in two categories, river dikes and sea dikes, which protect large cities like Amsterdam and Rotterdam.

There are four surrounding dike rings along the Western Scheldt. These dike rings are numbered from 29 to 32 in Fig. 5, and the plan view is shown in Fig. 1.The reliability assessment of this site is a defined task for the FloodSite project by utilizing limit state equations (LSEs). A large number of LSEs for different failure scenarios and failure modes were considered (Morris 2009) and their integration is addressed in (van Gelder 2009). These outcomes form the building blocks of this enormous project. In these studies, attempts have been made to define and apply LSEs for different failure modes of a usual flood defense structure, and most of the presented LSEs can be utilized for safety assessment. Among different failure modes, sliding is one of the important and influential failure modes that is difficult to model. This failure mode can be investigated by the analytical methods or finite

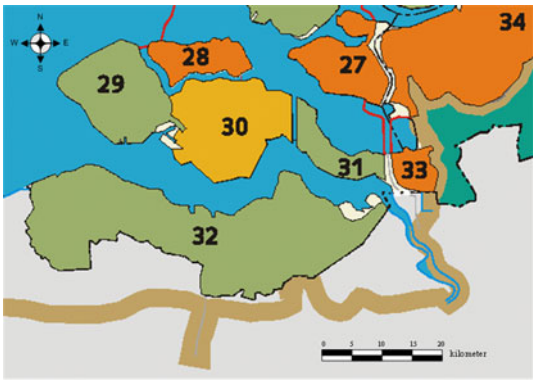

Fig. 5 Dike ring areas in the southern part of the province Zeeland are presented, this area is counted as number 32

element (FE) models. Since the reliability assessment of the FE models is a complicated and time-consuming process (Rajabalinejad et al. 2007; Aven 2007), analytical models can be used to compute failure probabilities. The outcome is used in PCRing, a reliability tool that takes into account effects of different parameters to assess safety of the entire dike ring. This program is developed by the Dutch ministry of water and transportation[2]. This process next to improve the safety assessment system of dike rings.

7 Model

The dike ring at Zeeuws-Vlaanderen, counted as dike ring 32, was initially divided into 287 dike sections. Approximately 33 dike and 4 dune sections are deemed to be representative for the total dike ring. This number does not include the water retaining structures (14 structures). The location of selected dike sections is shown in Fig. 6. Because calculation of the sliding mechanism is an elaborate process, it was not performed for all sections. The district water board selected seven cross-section profiles (out of a series of 40 that were used for the testing) during the process of schematization. These seven Profiles are selected for calculating the probabilities of failure for the sliding failure mechanism with MproStab software. Analysis of two typical sections is addressed next. Additional information is presented in (van Gelder 2009).

7.1 Section ALS166B

ALS166B is located on the North East of Dike Ring 32 (Fig. 6), the cross-section shown in Fig. 7 is a typical cross-section of the dike ring in Zeeland. The available data for this area are geometrical and geotechnical information. The soil layers are horizontal as shown in Fig. 7. The material properties of this section of the dike ring are provided in Table 1. The material numbers of in Table 1 correspond to the soil numbers in Fig. 7.

The main part of this dike is composed of sand and the downstream toe is made of clay. The foundation is sand with layers of peat[3] and loose clay[4] under the body of dike. The main parameters of soil layers are considered as random variables with a mean value,

[2] http://www.rijkswaterstaat.nl.

[3] In the original report is known as *Veen*.

[4] In the original report is known as *Slapkle*.

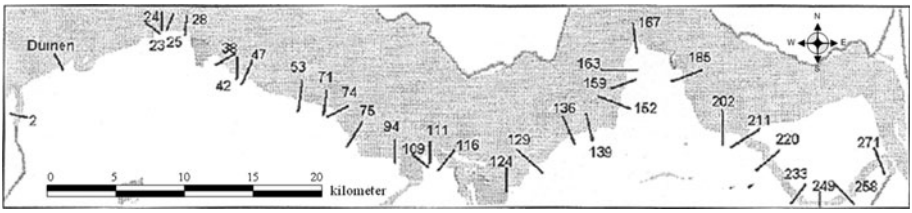

Fig. 6 Selected cross-sections of the dike ring in Zeeuws-Vlaanderen

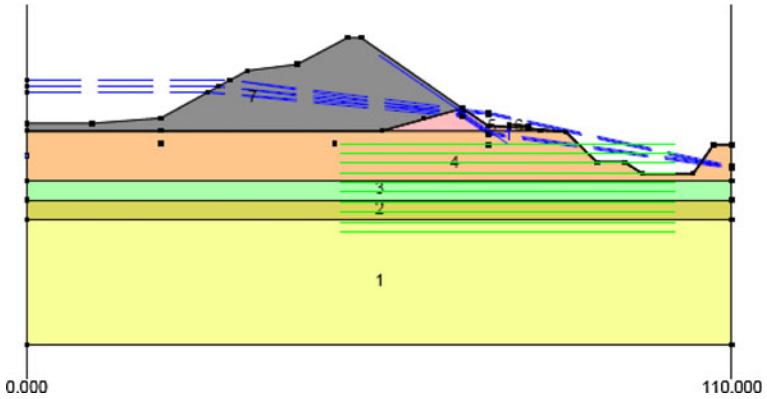

Fig. 7 The cross-section ALS166B used in the finite element model. The horizontal and vertical scales are different in this figure for clarification purpose

Table 1 Variation of soil parameters for section ALS166B, layer numbers are according to Fig. 7

Material number Material name	1 Sand	2 Hum-clay	3 Peat	4 Soft clay	5 Clay-dike	7 Sand-dike
Distribution$_c$	Logn	Logn	Logn	Logn	Logn	Logn
Distribution$_\phi$	Logn	Logn	Logn	Logn	Logn	Logn
γ_{dry}	17.00	13.00	12.00	14.00	17.00	17.00
γ_{sat}	20.00	13.00	12.00	14.00	17.00	20.00
μ_c	0.00	0.00	2.40	0.00	13.00	0.00
μ_ϕ	36.50	17.30	17.00	20.10	18.90	29.50
σ_c	0.00	0.00	0.65	0.00	3.60	0.00
Horizontal fluctuation scale (c)	50.00	50.00	50.00	50.00	50.00	50.00
Horizontal fluctuation scale (ϕ)	50.00	50.00	50.00	50.00	50.00	50.00
Vertica fluctuation scale (ϕ)	0.25	0.25	0.25	0.25	0.25	0.25
Variance ratio (ϕ)	0.75	0.75	0.75	0.75	0.75	0.75

standard deviation and a distribution type are presented in Table 1. This table presents the required data for stochastic Bishop analysis. This analysis and its required parameters shown in Table 1 are further explained in Sect. 4.

7.2 Section EMMA118

The other cross-section of Dike Ring 32 in the middle North is EMMA118, it is shown in Fig. 8 in a finite element model. This cross-section and its materials are similar to those of ALS166B. The description of the soil parameters for this cross-sections is addressed in (Rajabalinejad and van Gelder 2007). The reliability analysis of this section is similar to the previous section, except that this cross-section is less sensitive to the *model factor*. This parameter is described in Sect. 5.

8 Results of FORM

The outcomes of the first-order reliability method (FORM) applied to the Section 166B are shown in Table 2 for different model factors. These show that the two key variables in the failure of dike are the mean value and variation of the soil parameters for cohesion and the friction angle.

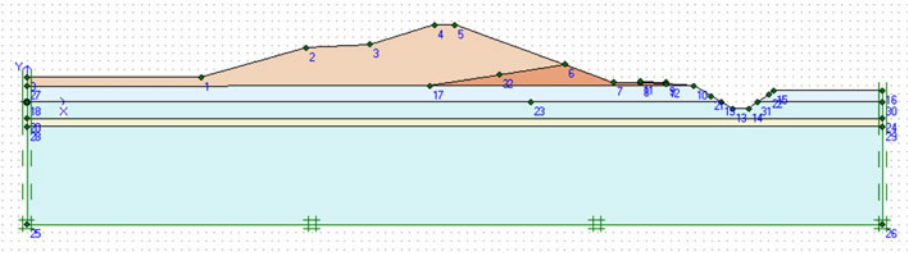

Fig. 8 Cross-section of EMMA118 as is modeled with finite elements. It is a typical cross-section of the dike in the Zeeuws-Vlaanderen, numbered as EMMA118

Table 2 Computation of index of reliability including the effect of randomness of extreme water levels for Section ALS166B by Mprostab

Model factor is 1		Model factor is 0.9	
Design value high water	5.396	Design value high water	5.396
Number of iterations	7	Number of iterations	7
α			
Fluctuation cohesion	0.123	Fluctuation cohesion	0.472
Uncertainty average value cohesion	0.155	Uncertainty average value cohesion	0.615
Fluctuation tan(ϕ)	0.529	Fluctuation tan(ϕ)	0.331
Uncertainty average value tan(ϕ)	0.823	Uncertainty average value tan(ϕ)	0.527
Correlation cohesion and tan(ϕ)	0.000	Correlation cohesion and tan(ϕ)	0.000
Uncertainty excess pore pressure	−0.000	Uncertainty excess pore pressure	−0.000
Uncertainty freatic line	−0.053	Uncertainty freatic line	−0.108
Model uncertainty	0.000	Model uncertainty	0.000
Uncertainty water level	0.007	Uncertainty water level	0.001

9 Results of Monte Carlo method

Eight soil parameters are considered in the reliability analysis of the dike ring section ALS166B. These variables are provided in Table 1 and their variation is assumed based on the field investigation that previously was done at this pilot site. We performed a preliminary Monte Carlo analysis of the important variables. Our preliminary analysis of the site indicated that a relatively high number of simulations would be required to obtain reliable estimates. This proves that optimization methods would be required for a reasonable number of calculations in reliability analysis of this site. Based on preliminary calculations, the influential variables were ranked according to the product moment correlation and rank correlation methods. The importance of having a ranking criteria in the DB method is described in (Rajabalinejad 2009; Rajabalinejad et al. 2008).

Here, we use the product moment correlation and the rank correlation (Rajabalinejad et al. 2010b). On the other hand, it is important to note that because of the nature of the finite element analysis, we obtain two sets of data for the failure and stability. We use the $c - \tan(\phi)$ method to obtain the safety factors when the model is stable. However, if the model is not stable for a certain condition, we calculate the ratio of the loading before the model fails. Therefore, the finite element model behaves like a bi-functional model. We call this the model behavior in the failure domain as "under threshold[5]" and the model behavior in the stable domain as "above threshold". This fact suggests investigating the influential variables for both of these domains. Results of the preliminary Monte Carlo simulation for the failure domain and the ranked influential variables are shown in Table 3. These show that there is an agreement between two ranking methods for selecting the first three or five influential variables. However, there are some differences in outcomes where the correlation values are close. Table 3 results indicate that the hum clay is the most influential variable and the sand dike and slap clay are the followings.

The influential variables in the stable domains are shown in Table 4. There is a strong correlation between the results of the rank correlation and product moment correlation for both their values and rankings. Nevertheless, there are differences between the results of Tables 3 and 4. For instance, for the first three influential variables, the role of sand dike in the failure process is more important than its role in the stability process.

The correlation among the basic and output variables are presented in the cobwebs plot in Fig. 9. The correlation of the percentage of loading (ms) in the failure domain, and the safety factor (fs) with the basic variables, is shown in Fig. 9a, b, respectively.For clarification purpose, the scatter plots of the calculated safety factors in the stable domain for two different variables are shown. Figure 10a shows a strong correlation between the hum clay layer and the safety factors, while Fig. 9b shows a very weak and almost zero correlation between the sand layer and the safety factor.

10 Application of the DB method

We apply the DB method to the section ALS166B by starting with a one-dimensional problem and increase the dimensionality of the problem until we obtain an answer with a reasonable accuracy. We choose the first influential variable and with a few number of calculations, to obtain the probability of failure. In order to obtain the required number of

[5] The threshold value is one.

Table 3 Contribution of variables to failure by the product moment correlation and rank correlation

No.	Product moment correlation			Rank correlation		
	Variable name	Soil layer no.	Value	Variable name	Soil layer no.	Value
1	Hum clay	2	0.727	Hum clay	2	0.749
2	Sand dike	7	0.414	Sand dike	7	0.513
3	Slap clay	4	0.275	Slap clay	4	0.210
4	Peat (ϕ)	3	0.113	Clay dike (c)	5	0.084
5	Clay dike (ϕ)	5	0.078	Peat (ϕ)	3	0.060
6	Peat (c)	3	0.027	Peat (c)	3	0.037
7	Sand	1	0.017	Clay dike (ϕ)	5	0.005
8	Clay dike (c)	5	0.06	Sand	1	0.05

Variables are numbered according to Fig. 7

Table 4 Contribution of variables to the model stability by the product moment correlation and rank correlation

No.	Product moment correlation			Rank correlation		
	Variable name	Soil layer no.	Value	Variable name	Soil layer no.	Value
1	Hum clay	2	0.731	Hum clay	2	0.731
2	Slap clay	4	0.348	Slap clay	4	0.339
3	Peat (ϕ)	3	0.312	Peat (ϕ)	3	0.287
4	Sand dike	7	0.262	Sand dike	7	0.264
5	Peat (c)	3	0.168	Peat (c)	3	0.160
6	Sand	1	0.068	Sand	1	0.076
7	Clay dike (c)	5	0.047	Clay dike (c)	5	0.028
8	Clay dike (ϕ)	5	0.043	Clay dike (ϕ)	5	0.038

Variables are numbered according to Fig. 7

simulations, Eq. 18 is suggested (Waarts 2000 and Rajabalinejad 2009).This equation provides a relation of the relative standard error $\vartheta(.)$ of failure probability (or its coefficient of variation), $\vartheta(\hat{p}_{\mathrm{f}})$, with the number of calculation, N as

$$N \geq \frac{1}{\vartheta(\hat{p}_{\mathrm{f}})^2} \times \left(\frac{1}{\hat{p}_{\mathrm{f}}} - 1\right) \tag{18}$$

where $\hat{p}_{\mathrm{f}}$ is the estimated probability of failure. However, in the Monte Carlo simulation, an accepted tolerance is used for a desired accuracy. A tolerance value less or equal to 0.05 is used in engineering practice. In the next step, we select two influential variables according to Tables 3 and 4. Since selection of the first two variables from these tables gives different results, we start with Table 3. These are the hum clay and sand dike numbered respectively as 1 and 7. We apply the two-dimensional DB. Table 5 shows the results. But it is unclear whether two-dimensional DB provides the required accuracy or higher dimensions are necessary. To check whether the selected dimension in the DB method suffices, we use Eq. 19 and have

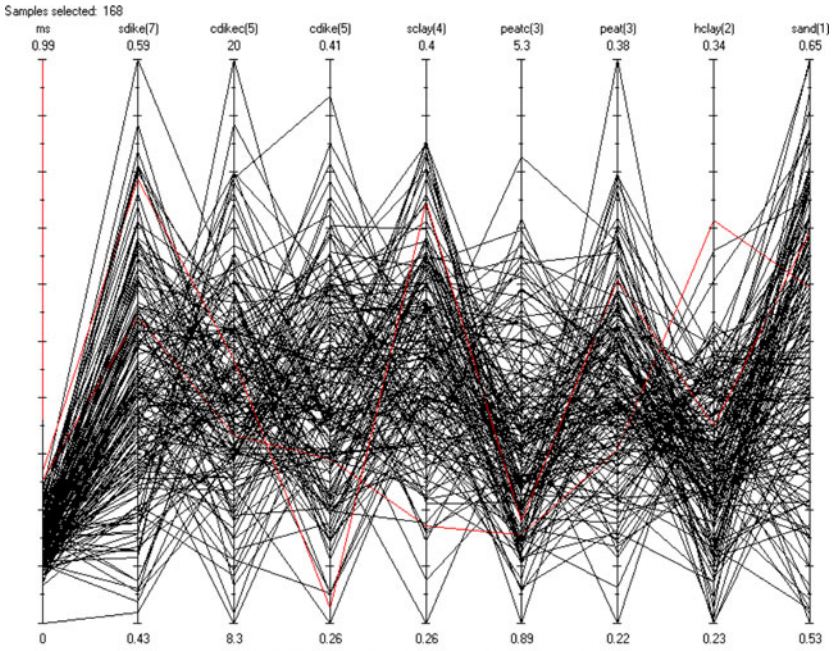

(a) Correlation in the failure domain

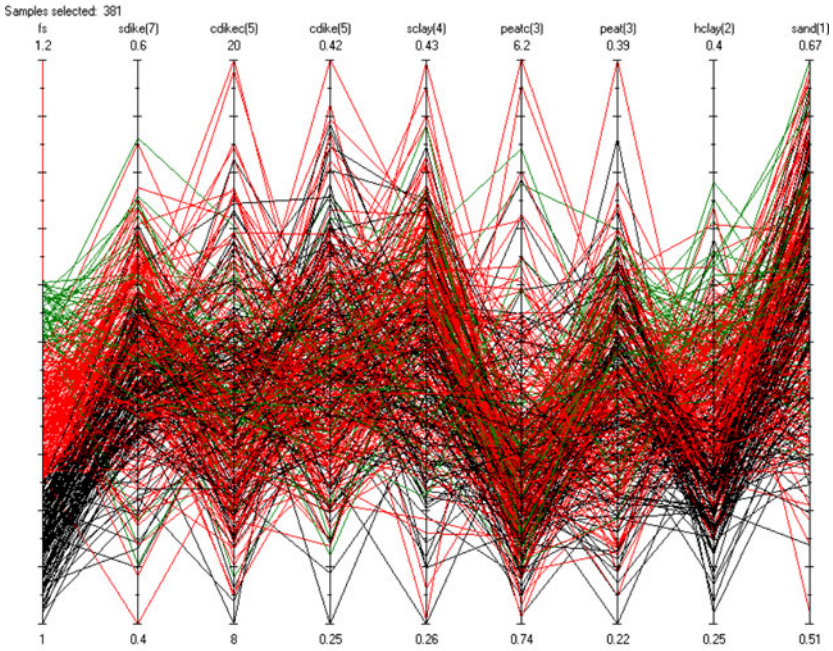

(b) Correlation in the stable domain

Fig. 9 Cobwebs graph of the variables to present the correlation among the variables and the corresponding safety factors for the failure and stable domain

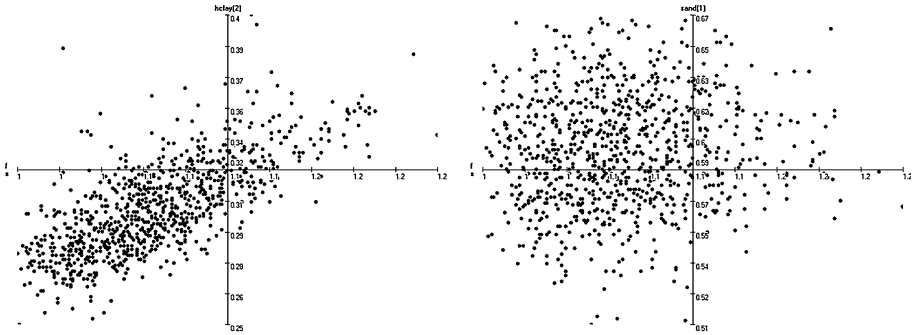

(a) safety factor versus hum clay layer **(b)** safety factor versus sand layer

Fig. 10 **a** shows the strong correlation of the hum *clay (2)* layer with the calculated safety factors; **b** shows a weak correlation of the sand *layer (1)* with the calculated safety factors

$$\widehat{DU_i} = \frac{\hat{p}_{\mathrm{f_i}} - \hat{p}_{\mathrm{f_{i-1}}}}{\hat{p}_{\mathrm{f_i}}} \tag{19}$$

In this equation, $\hat{p}_{\mathrm{f_i}}$ is the estimated probability of failure for the ith dimension of DB while $\hat{p}_{\mathrm{f_{i-1}}}$ is the probability of failure in the lower dimension.

The result from this equation presents uncertainty of the $(i-1)$th dimension of DB. Depending on the particulars of problems, it is necessary to use the maximum value of the dimensional uncertainty, DU_i. Then, one can obtain the required dimension for the DB method. It is important to note that DU_i approaches zero with increasing the dimensionality of the problem and becomes zero when all the variables in the Monte Carlo simulation are taken into account (DU_n). As a matter of fact, DU_i suggests the possible error by dimensionality of the problem and is different than using $\vartheta(.)$ in the Monte Carlo simulation. In other words, DU_i does not decrease if a high number of simulations were used in the ith-dimensional analysis. Since we ranked the variables according to their influence, DU_i ensures the rate of convergence for the Monte Carlo method. This parameter also depends on the combination of the input variables. It is important to note that DU_i is a random variable and may change by restarting the simulation. The standard deviation of this random variable can be calculated by

$$\sigma^2_{\widehat{DU_i}} \leq \frac{\sigma^2_{\hat{p}_{\mathrm{f_i}}} + \sigma^2_{\hat{p}_{\mathrm{f_{i-1}}}}}{{\hat{p}_{\mathrm{f_i}}}^2} \tag{20}$$

where σ is the standard deviation. This formula shows that $\sigma_{\widehat{DU}}$ is influenced by the related $\vartheta_i(.), \vartheta_{i-1}(.), \hat{p}_{\mathrm{f_i}}$ and $\hat{p}_{\mathrm{f_{i-1}}}$.

We check the sufficiency of two-dimensional analysis by Eqs. 19 and 20. Results in Table 3 have a coefficient of variation (COR) of 0.21. In other words, the dimensional uncertainty in the result obtained by a two-dimensional analysis is $\widehat{DU_2} = 0.21$. Since this is a relatively high COR, we proceed to a higher dimension by considering the next variable in Table 3, and include the variation of the slap clay layer and perform a three-dimensional analysis. We obtained $\widehat{DU_3} = 0.51$ that shows a high level of uncertainty. We include the next variable called peat in the four-dimensional DB and determined the dimensional uncertainty of $\widehat{DU_4} = 0.15$. To obtain a more accurate result, we considered to a higher level DB, where the dimensionality uncertainty reduces to $\widehat{DU_5} = 0.12$

Table 5 Results of DB method in different dimensions based on the contribution of variables to failure (Table 3)

No.	Dimension of DB	Number of DB simulations	Equivalent MC simulations	$\vartheta(.)$	$\widehat{DU}$	$\sigma_{\widehat{DU}}$
1	1D	3	4500	0.044		
2	2D	29	4500	0.050	−0.21	0.26
3	3D	115	4500	0.046	0.51	0.52
4	4D	280	4500	0.046	0.15	0.07
5	5D	397	4500	0.042	0.12	0.05

according to Table 5. One expects a monotonically decreasing DU by increasing dimension, and results obtained in Table 5 suggest an incorrect ranking of variables[6].

Since the influence of variables is an important issue in the DB method, we provide the correct choice for influential variables in Table 4. Because the first influential variable in Tables 3 and 4 is the same, we proceed to the two-dimensional analysis by considering the slap clay as the second variable. Result shows that the dimensional uncertainty at this level is $\widehat{DU}_2 = 0.36$, a relatively high COR. Next, we increase the dimension by including the peat material. The dimensional uncertainty reduces to 0.11 e.g. $\widehat{DU}_3 = 0.11$. For a higher accuracy, we include the sand dike material to get the dimensional uncertainty of $\widehat{DU}_4 = 0.04$. This is an acceptable value, and we conclude that four-dimensional analysis of this problem with four influential variables in Table 4 is necessary to achieve the desired accuracy. Our goal was to show for this problem that four correctly chosen influential variables were required to minimize the uncertainty in the calculation of probability of failure. In this case, we have

$$\frac{\rho_2 + \rho_4 + \rho_3 + \rho_7}{\rho_1 + \rho_2 + \cdots + \rho_8} = 0.84 \tag{21}$$

where ρ_i is the correlation between the ith variable and the output variable[7].

11 Discussion

Results are provided for two typical cross-sections of the Scheldt dike ring 32 described in Sect. 7. A comparison of different failure shapes for sections ALS166B and EMMA118 is presented in Fig. 11. Results from the stochastic Bishop with two different model factors are compared to results by the finite element method. We demonstrate in Fig. 11 the influence of model factor on the failure shape. The outcome can be almost independent of the model factor as is shown in Fig. 11 a, c or influenced by the model factor as is shown in Fig. 11b, d. Results in Fig. 11 do not support assumption of a circular failure shape as is considered for the Bishop method. This finding is important because many reliability programs for safety assessment of dikes and coastal structures use this technique. For instance, PCRing that is developed to assess the total safety of dikes in the Netherlands is

[6] This could be as a result of the fact that the number of simulations in failure domain is less than the number of simulations in stable domain.

[7] Using the rank correlation or product moment correlation, this ratio is almost the same. For further information, see (Rajabalinejad et al. 2010b).

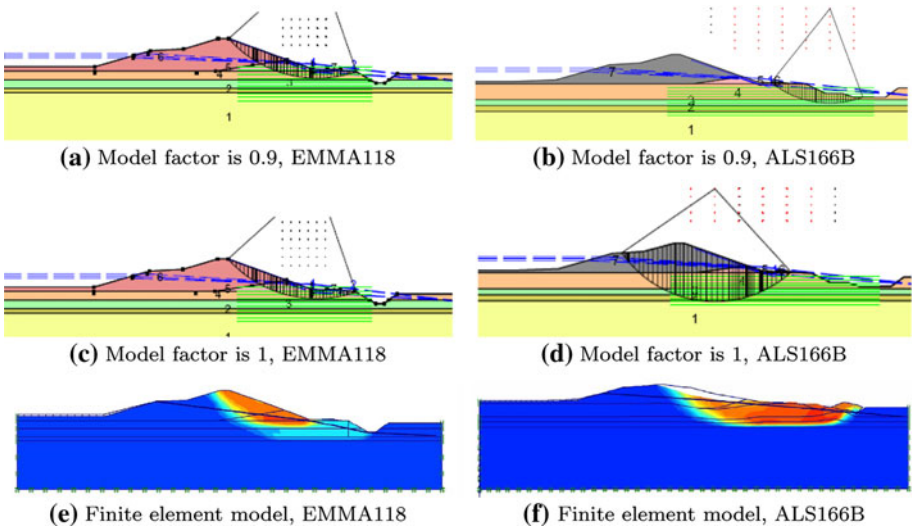

Fig. 11 Left-hand side figures are related to the cross-section EMMA118, and the right-hand side figures are related to the cross-section ALS166B. Sensitivity of the cross-section ALS166B to the model factor parameter in the stability analysis is considerable

fed by this technique for the sliding mechanism. Therefore, a more accurate technique for the reliability assessment of these infrastructures is required. We consider the finite element technique to be the best candidate. However, in order to fully utilize the advantages of the finite element model and make it affordable, the DB method is necessary. For this method, it is important to correctly rank the influential variables of a problem. The product moment correlation or rank correlation may be used for this purpose (Rajabalinejad et al. 2010b). The graphs like cobwebs shown in Fig. 9 are helpful for examining the nonlinear correlations. It is also important to choose the required dimension for a desired accuracy. We introduced in this paper the dimensional uncertainty ($\widehat{DU}_i$) by Eq. 19. The DU_i can be used to determine whether or not the ith dimension can fulfill the desired accuracy.

A comparison of results in Table 5 and Table 6 clearly shows that different combination of variables produces different values of failure probability and dimensional uncertainty. This is the consequence of the importance of ranking influential variables in the DB method. For a proper ranking, we implemented the bi-functional response of the finite element model using the product moment correlation and rank correlation for both stable

Table 6 Results of DB method in different dimensions based on the contribution of variables to failure (Table 4)

No.	Dimension of DB	Number of DB simulations	Equivalent MC simulations	$\vartheta(.)$	$\widehat{DU}$	$\sigma_{\widehat{DU}}$
1*	1D	3	4500	0.044		
2	2D	12	4500	0.039	0.36	0.048
3	3D	65	4500	0.042	−0.11	0.06
4*	4D	280	4500	0.046	0.04	0.062

* This row is identical to the same row in Table 5

and failure domains. For the stable domain, the agreement between two different ranking methods of the product moment correlation and rank correlation for the stable domain is good as shown in Table 4. We also observed that the correlation of variables in the stable domain constantly leads to more uniform and better results.

After a series of calculation, we determined that 65 simulations were enough to reach the required accuracy for four variables shown in Table 4. We determined the number of simulations in each series of simulations using different number of variables. On the other hand, the DB results can be stored on the stable or failure bounds for the next series of simulations, and this will further reduce the number of simulations required. This is obvious by a comparison of the number of simulations in Tables 5 and 6. For instance, in a two-dimensional and three-dimensional DB, 29 and 115 simulations were required, respectively, that have been reduced to 12 and 65, accordingly.

12 Conclusions

For the safety assessment of flood defense systems, the stochastic Bishop is currently applied to the pilot site Scheldt. This widely used technique is a straightforward and relatively fast process, requires fewer parameters in comparison with the finite element method. However, we show in this paper that results of this method in some cases could be unreliable and misleading. We demonstrate the influence of the model factor on the safety assessment process by examples. Our results indicate that a close attention must be paid to the outcomes of this method and compared with finite element models. In particular, it could be prudent to check and confirm the results obtained for the failure surface or safety factor for flood defense systems.

In general, the finite element method is a much more accurate technique for the failure assessment of the dike rings. To make this technique affordable in the safety assessment process, the dynamic bounds method is described here in circumstances with a bi-functional response implemented in the finite element model. Our results indicated that better correlation ratios can be obtained by separating the response of the finite element model in the stable and failure domains. For this case study, the controlling variables in the stable domain produced better results. Additional investigations are necessary in different case studies before our proposed method can be used in practical applications as a standard. We also observed that a four-dimensional DB analysis with 85% of the influential variables provided the desired accuracy.

In this study, we introduced the concept of dimensional uncertainty (*DU*) for the DB method in order to determine the required dimensionality of simulations. We treated the *DU* as a random variable by its expected value and standard deviation or variation. Our next goal is to establish a direct relation between the correlation ratio of the input variables and the dimensional uncertainty in a given application.

Acknowledgments Authors acknowledge Dr. Zeki Demirbilek, US Army R&D Center in Vicksburg/USA, for his valuable advice and contributions to this paper, and express our deep appreciation for his help.

References

Aven T (2007) In: European safety and reliability conference (ESREL 2007) Jun 25–27, 2007 University Stavanger, Stavanger

Baker R, Garber M (1978) Theoretical-analysis of stability of slopes. Geotechnique 28(4):395–411

Calle EOF (1994) Mprostab user's guide. Geodelft, Delft

Choi SK, Grandhi RV, Canfield RA (2006) Reliability-based structural design. Springer, Berlin
Demirbilek Z, Lin L, Mark D (2009) Chesapeake bay storm flooding frequency-of-occurrence studies. Tech. rep., U.S. Army Engineer Research and Development Center
Vicksburg MS (2008) Numerical modeling of storm surge in Chesapeake Bay. Intl J Ecol Dev 10:24–39
Demirbilek Z, Resio D, Dean R (2010) A forensic analysis of hurricane Katrina's impact: methods and findings. Special Issue, Ocean Eng 37(1):154
Fishman GS (1996) Monte Carlo: concepts, algorithms, and applications. Springer, Berlin
FloodSite (2004–2009) Integrated flood risk analysis and management methodologies. http://www.floodsite.net
Griffiths DV, Fenton GA (2007) Probabilistic methods in geotechnical engineering, vol I. Springer, Wien
Griffiths DV, Lane PA (1999) Slope stability analysis by finite elements. Geotechnique 49(3):387–403
Haldar A, Mahadevan S (2000) Reliability assessment using stochastic finite element analysis. Wiley, New York
Lacasse S, Nadim F, Uzielli M (2007) Hazard and risk assessment of landslides. Geotechnical Special Publication (157)
Link LE, Jaeger JJ, Stevenson J, Stroupe W, Mosher RL, Martin D, Garster JK, Zilkoski DB, Ebersole BA, Westerwink JJ (2006) Performance evaluation of the new orleans and southeast louisiana hurricane protection system: Draft final report of the interagency performance evaluation task force, vol 1. United States Army Corps of Engineers (USACE), vols 1e9 (2006)
Malkawi AIH, Hassan WF, Abdulla FA (2000) Uncertainty and reliability analysis applied to slope stability. Struct Saf 22(2), 161–187. 330GM Times Cited:9 Cited References Count:25
Melchers RE (1999) Structural reliability analysis and prediction, 2nd edn. Wiley, Chichester. 98053106 GB99-20653, Robert E. Melchers. ill.; 26 cm. Includes bibliographical references (pp 409–430) and index.
Morris M (2009) Understanding and predicting failure modes. Tech. rep., HR Wallingford Ltd (2009). http://www.floodsite.net
Nie J, Ellingwood BR (2000) Directional methods for structural reliability analysis. Struct Saf 22(3):233–249
Rajabalinejad M (2009) Reliability methods for finite element models. IOS Press, Amsterdam.
Rajabalinejad M (2010) Bayesian Monte Carlo method. Reliab Eng Syst Safe 95(10):1050–1060. doi:10.1016/j.ress.2010.04.014
Rajabalinejad M, Mahdi T (2010) The inclusive and simplified forms of Bayesian interpolation for general and monotonic models using Gaussian and generalized beta distributions with application to Monte Carlo simulations. Nat Hazards. doi:10.1007/s11069-010-9560-3
Rajabalinejad M, van Gelder P (2007) Application of probabilistic finite elements in geotechnical engineering. Tech. rep., Technical University Delft. http://www.floodsite.net
Rajabalinejad M, Kanning W, van Gelder P, Vrijling JK, van Baars S (2007) Probabilistic assessment of the flood wall at 17th street canal, new orleans. Risk, Reliability and Societal Safety, vols 1–3, pp 2227–2234
Rajabalinejad M, van Gelder P, Vrijling JK (2008) Probabilistic finite elements with dynamic limit bounds: a case study: 17th street flood wall, New Orleans. 6th International Conference on Case Histories in Geotechnical Engineering and Symposium in Honor of Professor James K. Mitchell, Rolla, Missouri University of Science and Technology, Missouri, USA
Rajabalinejad M, van Gelder P, Vrijling JK (2009) Stochastic methods for safety assessment of a European pilot site: Scheldt. Geotechnical Risk and Safety, Gifu, Japan, Taylor & Francis Group, London
Rajabalinejad M, Demirbilek Z, Mahdi T (2010a) Determination of failure probabilities of flood defence systems with improved dynamic bounds method. Nat Hazards. doi:10.1007/s11069-010-9561-2
Rajabalinejad M, van Gelder P, Demirbilek Z, Mahdi T, Vrijling, JK (2010b) Application of the dynamic bounds method in the safety assessment of flood defences, a case study: 17th street flood wall, New Orleans. Georisk: Assessment and Management of Risk for Engineered Systems and Geohazards. doi:10.1080/17499510903416170
Smith I, Griffiths D (2004) Programming the finite element method. Wiley, New York
USACE-b (2006) Orleans and Southeast Louisiana Hurricane Protection System, Volume II Geodetic Vertical and Water Level. Tech. Rep. 167, U.S. Army Corps of Engineers, Report of the Interagency Performance Evaluation Task Force
van Gelder P (2009) Reliability analysis of flood defense systems. Tech. rep., Technical University Delft, Delft. http://www.floodsite.net
van Gelder P, Mai CV, Wang W, Shams G, Rajabalinejad M, Burgmeijer M (2008) Data management of extreme marine and coastal hydro-meteorological events. J Hydraul Res 46(2):191–210
Vanmarcke E (1983) Random fields analysis and synthesis. MIT Press, Cambridge, MA
Waarts P (2000) Structural reliability using finite element analysis. Ph.D. thesis, Delft University of Technology, Delft, 189 pp